Surface Integrated Field Equations Method for computing 3D static and stationary electric and magnetic fields

Zhifeng Sheng* Patrick Dewilde† Rob Remis‡

Abstract — **This paper describes how the Surface Integrated Field Equations method (SIFE) is used to compute 3D static/stationary electric and magnetic fields in which high contrast materials occur. It gives an account of the promising results that are obtained with it when compared to traditional approaches. Advantages of the method are the improved flexibility and accuracy for a given discretization level, at the cost of higher computational complexity.**

1 Introduction

In our previous work, we have used the Surface Integrated Equations method for solving 2D electromagnetic problems in the time domain[1, 2] and 3D electromagnetic problems in the time domain[3], in which regions are present that exhibit highly contrasting material properties (electric and/or magnetic) with each other. In this paper, we develop the method to compute 3D static electric and magnetic fields. When the EM field quantities do not vary with time, the time-derivative of the fields quantities vanishes, and we have a static or stationary field. In these cases, there is no interaction between electric field and magnetic field, so that the electro-stationary, electrostatic and magnetostatic case can be solved individually in one generic system. The surface integrated equations derived for the static and stationary electric and magnetic fields have the same form. Therefore we may represent all such field equations in a generic form as shown in Tab. 1. Let $\mathcal{D}$ be the domain of interest with boundary $\partial\mathcal{D}$ and let S be any surface ($S \in \mathcal{D}$) with boundary ∂S. The generic surface integrated field equation is

$$\oint_{\partial S} \mathbf{V}(\mathbf{x}) \cdot \mathrm{d}\mathbf{l} \quad = \quad \int_S \mathbf{Q}^{\mathrm{imp}}(\mathbf{x}) \cdot \mathrm{d}\mathbf{A} \qquad (1)$$

Although we can deal with more complicated relations, in this paper we consider only linear, non-dynamic media characterized by

$$\mathbf{F}(\mathbf{x}) = \xi(\mathbf{x})\mathbf{V}(\mathbf{x}) \qquad (2)$$

*Circuits and Systems, EEMCS, Mekelweg 4 2628 CD Delft, The Netherlands, e-mail: z.sheng@ewi.tudelft.nl.

†Circuits and Systems, EEMCS, Mekelweg 4 2628 CD Delft, The Netherlands, e-mail: p.dewilde@ewi.tudelft.nl.

‡Laboratory of Electromagnetic Research, EEMCS, Mekelweg 4, 2628 CD Delft, The Netherlands, e-mail: r.f.remis@tudelft.nl.

Let $\mathcal{V}$ be any volume in $\mathcal{D}$ with boundary $\partial\mathcal{V}$, the generic compatibility relation that applies for static and stationary electric and magnetic fields in the surface integrated form is

$$\oint_{\partial\mathcal{V}} \mathbf{F}(\mathbf{x}) \cdot \mathrm{d}\mathbf{A} \quad = \quad \oint_{\mathcal{V}} \rho^{\mathrm{imp}}(\mathbf{x})\mathrm{d}V. \qquad (3)$$

Let $\mathcal{I} \in \mathcal{D}$ be the interfaces of discontinuity, the interface conditions are:

$$\nu \times \mathbf{V}(\mathbf{x})|_1^2 \quad = \quad \mathbf{Q}_S^{\mathrm{imp}}(\mathbf{x}), \mathbf{x} \in \mathcal{I} \qquad (4)$$

$$\nu \cdot \mathbf{F}(\mathbf{x})|_1^2 \quad = \quad \sigma^{\mathrm{imp}}(\mathbf{x}), \mathbf{x} \in \mathcal{I} \qquad (5)$$

where $\nu \times \mathbf{V}(\mathbf{x})$ denotes the tangential component of the field strength across the interface, $\nu \cdot \mathbf{F}(\mathbf{x})$ denotes the normal component of flux density accross the interface. As for boundary conditions, let $\partial\mathcal{D}^H \cup \partial\mathcal{D}^E = \partial\mathcal{D}$ and $\partial\mathcal{D}^H \cap \partial\mathcal{D}^E = \emptyset$, we have:

$$\nu \times \mathbf{V}(\mathbf{x}) \quad = \quad \nu \times \mathbf{V}^{\mathrm{ext}}(\mathbf{x}), \mathbf{x} \in \partial\mathcal{D}^V \qquad (6)$$

$$\nu \cdot \mathbf{F}(\mathbf{x}) \quad = \quad \sigma^{\mathrm{ext}}(\mathbf{x}), \mathbf{x} \in \partial\mathcal{D}^F. \qquad (7)$$

where $\nu \times \mathbf{V}^{\mathrm{ext}}(\mathbf{x})$ denotes the tangential component of the field strength on the exterior boundary, $\sigma^{\mathrm{ext}}(\mathbf{x})$ denotes the normal component of the electric current density, the electric flux density or magnetic flux density on the exterior boundary.

2 Discrete field equations

In this section, we replace the continuous field quantities in the generic field equations for static and stationary electric and magnetic fields, presented in Sec. 1, with their discrete linear counterparts to derive a system of linear, algebraic equations in terms of unknown coefficients (degrees of freedom). In the SIFE method for computing static and stationary electric and magnetic fields, we want the linearly approximated field quantities to satisfy Eq. (1) and Eq. (3) at the bounding surfaces of each elemental volume. Moreover, the approximated field must comply with the interface conditions Eq. (4), Eq. (5) and boundary conditions Eq. (6), Eq.(7). Before introducing the discretized field equations, we define a few geometrical quantities (see Fig. 1). Let a tetrahedron with global

978-1-4244-3386-5/09/$25.00 ©2009 IEEE

Table 1: Correspondence between generic quantities and the actual static and stationary field values

Generic form	stationary electric case	static electric case	stationary magnetic case
$\mathbf{V}$	$\mathbf{E}$	$\mathbf{E}$	$\mathbf{H}$
$\mathbf{F}$	$\mathbf{J}$	$\mathbf{D}$	$\mathbf{B}$
ξ	σ	ε	μ
$\mathbf{Q}^{\text{imp}}$	0	0	$\mathbf{J}^{\text{tot}}$
$\mathbf{Q}_S^{\text{imp}}$	0	0	$\mathbf{J}_S^{\text{imp}}$
ρ^{imp}	$-\nabla\cdot\mathbf{J}^{\text{imp}}$	ρ	0
σ^{imp}	$-\nu\cdot\mathbf{J}^{\text{imp}}\Big\vert_1^2$	σ_e	0
$\mathbf{V}^{\text{ext}}$	$\mathbf{E}^{\text{ext}}$	$\mathbf{E}^{\text{ext}}$	$\mathbf{H}^{\text{ext}}$
σ^{ext}	$\nu\cdot\mathbf{J}^{\text{ext}}$	$\nu\cdot\mathbf{D}^{\text{ext}}$	$\nu\cdot\mathbf{B}^{\text{ext}}$

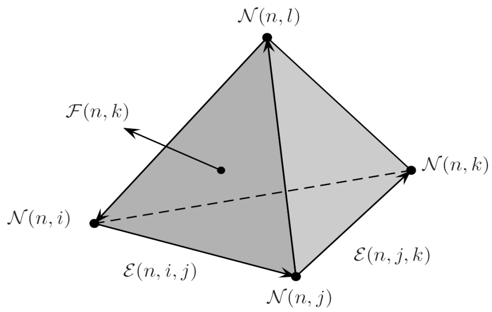

Figure 1: Tetrahedron $\mathcal{T}(n)$. (i,j,k,l) correspond to a right oriented system of edges $(i,j),(i,k),(i.l)$.

tetrahedron index n be denoted as $\mathcal{T}(n)$. We denote the four nodes delimiting $\mathcal{T}(n)$ locally as $\mathcal{N}(n,i), i=\{0,1,2,3\}$. Let $\mathcal{E}(n,i,j), j\neq i$ be the edge pointing from $\mathcal{N}(n,i)$ to $\mathcal{N}(n,j)$, and $\mathbf{e}(n,i,j)$ be the vectorial length of the edge $\mathcal{E}(n,i,j)$. Let $\mathcal{F}(n,k), k=\{0,1,2,3\}$ be a facet of tetrahedron $\mathcal{T}_n$, which is not delimited by the node $\mathcal{N}(n,k)$, and $\mathbf{A}(n,k)$ be the vectorial area of the facet $\mathcal{F}(n,k)$, e.g.

$$\mathbf{A}(n,0) \quad = \quad \frac{1}{2}\left[\mathbf{e}(n,1,2)\times\mathbf{e}(n,2,3)\right].$$

Let $V(n)$ be the volume of the tetrahedron $\mathcal{T}(n)$, $\mathbb{T}$ be the set of tetrahedrons in the mesh and h the average length of edges in the mesh.

Definition 1. *we define: $\mathbb{N}_{\mathbf{V}}^C$ as the set of nodes on which $\mathbf{V}(\mathbf{x})$ is totally continuous, that is, the set of continuity nodes[3], and $\mathbb{N}_{\mathbf{V}}^D$ as the set of nodes on which $\mathbf{V}(\mathbf{x})$ is continuous in its tangential component and discontinuous in its normal component, that is, the set of discontinuity nodes[3]. We have*

$$\mathbb{N}=\mathbb{N}_{\mathbf{Q}}^C\bigcup\mathbb{N}_{\mathbf{Q}}^D,\ \mathbb{N}_{\mathbf{Q}}^C\bigcap\mathbb{N}_{\mathbf{Q}}^D=\emptyset,$$

Definition 2. *For $n\in\mathbb{I}_{\mathcal{T}}$ and $i\in\{0,1,2,3\}$,*

$$\mathbf{V}^{\mathcal{N}(n,i)}=\sum_{k=\{1,2,3\}}\left[V_k^{\mathcal{N}(n,i)}\mathbf{i}_k\right], \forall\mathcal{N}(n,i)\in\mathbb{N}_{\mathbf{V}}^C.$$

or

$$\mathbf{V}^{\mathcal{N}(n,i)} = \sum_{j=\{0,1,2,3\}j\neq i}\left[V^{\mathcal{E}(n,i,j)}\left(-\frac{|\mathbf{e}(n,i,j)|}{3V(n)}\mathbf{A}(n,j)\right)\right], \quad \forall\mathcal{N}(n,i)\in\mathbb{N}_{\mathbf{V}}^D$$

where $V_k^{\mathcal{N}(n,i)}$ and $V^{\mathcal{E}(n,i,j)}$ are the unknown linear expansion coefficients (degrees of freedom).

By discretizing Eq. (1) applied on every facet of every tetrahedron, we obtain

$$\begin{aligned}&\frac{1}{2}\mathbf{e}(n,l,k)\cdot\mathbf{V}^{\mathcal{N}(n,j)}+\frac{1}{2}\mathbf{e}(n,j,l)\cdot\mathbf{V}^{\mathcal{N}(n,k)}\\&+\frac{1}{2}\mathbf{e}(n,k,j)\cdot\mathbf{V}^{\mathcal{N}(n,l)}\\&=\sum_{h=j,k,l}\left[\frac{1}{3}\mathbf{A}(n,i)\cdot\mathbf{Q}^{\text{imp}}(\overline{\mathbf{x}}(n,h))\right],\end{aligned}\qquad(8)$$

By discretizing Eq. (3) applied on the bounding surface of every tetrahedron, we obtain:

$$\begin{aligned}&-\sum_{h=i,j,k,l}\left[\frac{1}{3}\mathbf{A}(n,h)\cdot\xi(\overline{\mathbf{x}}(n,h))\mathbf{V}^{\mathcal{N}(n,h)}\right]\\&=\sum_{h=i,j,k,l}\left[\frac{1}{4}V(n)\rho^{\text{imp}}(\mathbf{x}(n,h))\right],\end{aligned}\qquad(9)$$

where $n\in\mathbb{I}_{\mathcal{T}}$; (i,j,k,l) is an even permutation of $(0,1,2,3)$ and $\mathbf{V}^{\mathcal{N}(n,i)}$ is defined in Def. 2.

The interface condition Eq. (4) is satisfied exactly by the correct field interpolation. By discretizing Eq. (5) applied on every facet that is on the interfaces of discontinuity, we obtain

$$\begin{aligned}&\sum_{j=\{\text{j1,k1,l1}\}}\left[\frac{1}{3}\mathbf{A}(\text{n1},\text{i1})\cdot\xi(\overline{\mathbf{x}}(\text{n1},j))\mathbf{V}^{\mathcal{N}(\text{n1},j)}\right]\\&+\sum_{j=\{\text{j2,k2,l2}\}}\left[\frac{1}{3}\mathbf{A}(\text{n2},\text{i2})\cdot\xi(\overline{\mathbf{x}}(\text{n2},j))\mathbf{V}^{\mathcal{N}(\text{n2},j)}\right]\\&=\sum_{j=\{\text{j1,k1,l1}\}}\left[\frac{1}{3}\mathbf{A}(\text{n1},\text{i1})\sigma^{\text{imp}}(\mathbf{x}(\text{n1},j))\right],\end{aligned}\qquad(10)$$

Table 2: Configuration of the two sub-domains

$\mathcal{D}_i$	sub-domains	μ_r
$\mathcal{D}_0$	$0 \le x_1 < 0.5$ and $0 \le x_2 < 0.5$	1000
$\mathcal{D}_1$	$0.5 < x_1 \le 1$ or $0.5 < x_2 \le 1$	1

where $\mathcal{T}(\mathrm{n1}) \in \mathbb{T}$ and $\mathcal{T}(\mathrm{n2}) \in \mathbb{T}$, n1$\neq$n2. $\mathcal{T}(\mathrm{n1})$ and $\mathcal{T}(\mathrm{n2})$ share a same face locally labeled as $\mathcal{F}(\mathrm{n1,i1})$ in $\mathcal{T}(\mathrm{n1})$ and $\mathcal{F}(\mathrm{n2,i2})$ in $\mathcal{T}(\mathrm{n2})$, respectively. (i1,j1,k1,l1) and (i2,j2,k2,l2) are both even permutations of $(0,1,2,3)$. There exists $j \in$ {j1,k1,l1} such that $\mathcal{N}(n1,j) \in \mathbb{N}^D_{\mathbf{V}}$.

We implement the boundary condition Eq. (6) and Eq.(7) implicitly on each node of the boundary.

3 The least-squares method

With the equations (8), (9), (10), and the discrete boundary conditions, one can prove that the system of equations has more equations than unknowns. Such a system may have no solution at all. One thing we can do is to find an approximate solution which minimizes a quadratic functional representing the error. With the weighted least-squares method[4], we can easily construct a set of normal equations, which we then solve with an iterative method to obtain an approximated electromagnetic field strength in the domain of computation. The method is numerically stable because the normal equations are positive definite by construction.

4 Numeric experiments

We test the SIFE method on a (admittedly rare) example of a situation where at the same time there exists a theoretical solution. The configuration is a domain $\mathcal{D} = \{0 \le x_1 \le 1, 0 \le x_2 \le 1, 0 \le x_3 \le 0.5\}$,bounded by PEC boundary condition ($\nu \cdot \mathbf{B}(\mathbf{x}) = 0, \forall \mathbf{x} \in \partial\mathcal{D}$). $\mathbf{J}^{\mathrm{tot}}(\mathbf{x})$ is chosen such that the exact magnetic field strength is:

$$\mathbf{H}(\mathbf{x}) = \frac{\pi \sin(\pi x_1)\cos(\pi x_2)}{\mu(\mathbf{x})}\mathbf{i}_1 - \frac{\pi \cos(\pi x_1)\sin(\pi x_2)}{\mu(\mathbf{x})}\mathbf{i}_2$$

The electric current density in the domain is then

$$\mathbf{J}^{\mathrm{tot}}(\mathbf{x}) = \frac{2\pi^2 \sin(\pi x_1)\sin(\pi x_2)}{\mu(\mathbf{x})}\mathbf{i}_3$$

4.1 Configuration with high contrast

The computational domain consists of two homogeneous sub-domains as defined in Tab. 2. To show the necessity of hybrid finite elements, we compute the solution offered for this configuration by the SIFE method based on hybrid elements, the SIFE method based on nodal elements, and the weighted Galerkin method based on nodal elements. Fig. 2(a) shows the results. It is apparent that the SIFE method based on hybrid finite elements maintains the optimal convergence rate which is of order $O(h^2)$ in both sub-domains. However, nothing comes for free, as shown in Fig. 2(b), the BICG-stable linear iterative solver for the SIFE method based on hybrid finite elements has to use incomplete CC with fill level 2 to reach the same convergence (10^{-12}), otherwise the solution is very difficult to find. Fortunately, the order of computational cost does not change; still it is of order $O(h^{-2})$.

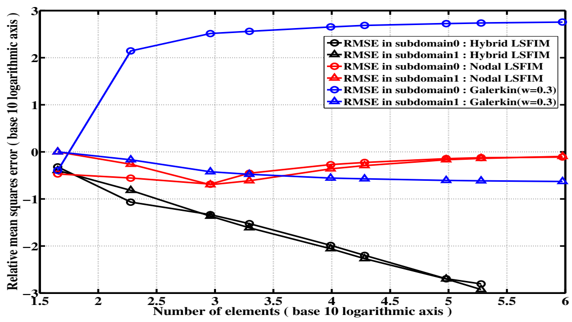

(a) convergence

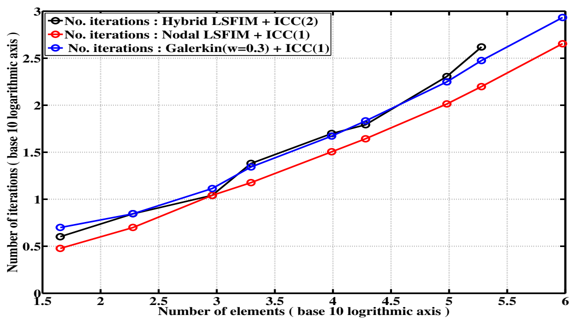

(b) computational cost

Figure 2: The RMSE($\mathbf{H}$) in the two sub-domains computed with different methods vs. the number of finite elements in the mesh (a).The number of iterations needed by different methods vs. the number of finite elements in the mesh. Bicg-stable method + nest dissection reordering + ICC(1)/ICC(2) (b).

4.2 Configuration with very high contrast

To test the limit of the SIFE method based on hybrid elements in handling extremely high contrast, we take the same configuration as that in Section 4.1, except now the relative permeability in homogeneous sub-domain 0 ranges from 1 to 1×10^{11}. A series of numeric experiments are conducted with

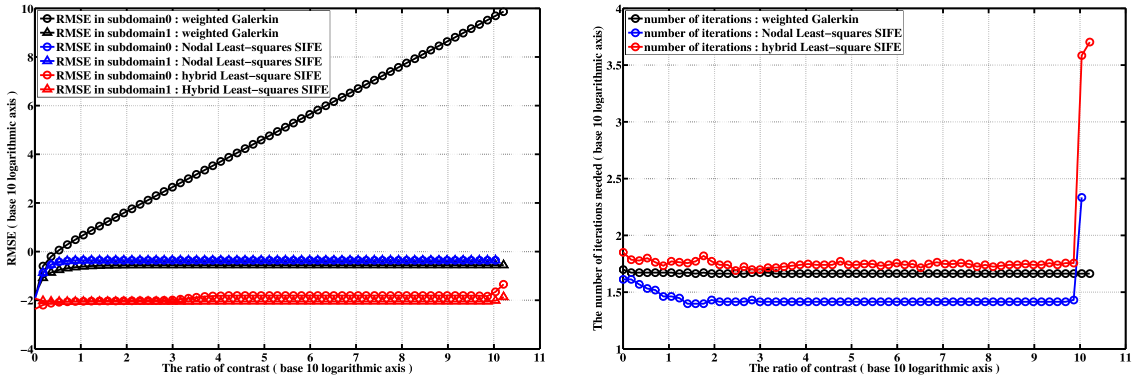

(a) convergence

(b) computational cost

Figure 3: The relative root mean square error in $\mathcal{D}_0$ and $\mathcal{D}_1$ vs. the ratio of contrast (a). The number of iterations needed by iterative linear solvers versus the ratio of contrast; BICG-stable + nested dissection reordering + ICC(2). the accuracy of the iterative linear solver: 1×10^{-12}(b).

the same interface conforming mesh. We show the comparison between the SIFE method based on hybrid elements with the SIFE method based on nodal elements and the weighted (w=0.3) Galerkin method based on nodal elements. As shown in Figure 3(a), as the ratio of contrast increases, the solution computed with the SIFE method based on hybrid elements stays stable and accurate in both subdomain 0 and sub-domain 1. The solution becomes inaccurate in the case of extremely high contrast 10^{12}, because we implemented the boundary condition implicitly. With the presence of extremely high relative permeability, some off-diagonal entries of the system matrix obtained by the SIFE method based on hybrid elements are comparable with the weighting factor for the implicit boundary conditions, which is approximately 10^{20}. In these extreme cases, the implicit boundary conditions will fail and the system matrix is close to singular. The same phenomena can be observed in Fig. 3(b). The computational costs for the SIFE method based on hybrid elements is higher than for the other two methods. However, the computational cost of the SIFE method based on hybrid elements does not increase with the contrast ratio.

5 Conclusions

The SIFE method holds considerable promise to solve three dimensional static and stationary electric and magnetic problems, in which high contrasts between different types of materials exist and irregular structures are present. It handles irregular structures and partial discontinuities in a systematically correct and elegant fashion. Its accuracy and stability are demonstrated and verified with numerical experiments. A EM simulation software has been implemented with OO C++.

Acknowledgments

The authors gratefully acknowlege the support from the Technology Foundation STW under the MICES project. The authors hereby acknowledge Prof. A.T. de Hoop for providing the central idea (the use of edge elements) of the paper.

References

[1] Zhifeng Sheng, Rob Remis, and Patrick Dewilde, “A least-squares implementation of the field integrated method to solve time domain electromagnetic problems,” *Computational Electromagnetics in Time-Domain, 2007. CEM-TD 2007. Workshop on*, pp. 1–4, 15-17 Oct. 2007.

[2] Z. Sheng, P.M. Dewilde, and R.F. Remis;, “The field integrated method to solve time domain electromagnetic problems,” in *IEEE/ProRISC workshop on Circuits, Systems and Signal Processing, Veldhoven (NL), IEEE,*, November 2007.

[3] Z. Sheng, P.M. Dewilde, and R.F. Remis;, “Surface integrated field equations method for solving 3d electromagnetic problems,” in *Scientific Computing in Electric Engineering, Helsinki University of Technology, Finland, 2008,*, Sept. 28-Oct. 3, 2008.

[4] BO-NAN Jiang, *The Least-Squares Finite Element Method: Theory and Applications in Computational Fluid Dynamics and Electromagnetics (Scientific Computation)*, 2006.